

Extinction radial profiles of M83 from GALEX UV imaging

Samuel Boissier¹, Armando Gil de Paz¹, Barry F. Madore^{1,2}, Alessandro Boselli³,
Véronique Buat³, Denis Burgarella³, Peter G. Friedman⁴, Tom A. Barlow⁴, Luciana
Bianchi⁵, Yong-Ik Byun⁶, José Donas³, Karl Forster⁴, Timothy M. Heckman⁷, Patrick N.
Jelinsky⁸, Young-Wook Lee⁶, Roger F. Malina³, D. Christopher Martin⁴, Bruno Milliard³,
Patrick Morrissey⁴, Susan G. Neff⁹, R. Michael Rich¹⁰, David Schiminovich⁴, Oswarld H.
W. Sigmund⁸, Todd Small⁴, Alex S. Szalay⁷, Barry Y Welsh⁸, and Ted K. Wyder⁴

ABSTRACT

We use the far-UV (FUV) and near-UV (NUV) images of M83 obtained by GALEX to compute the radial profile of the UV spectral slope in the star forming disk. We briefly present a model of its chemical evolution which allows us to obtain realistic intrinsic properties of the stellar populations. Using corollary data, we also compute the profiles of $H\alpha/H\beta$ and of the total IR (TIR) to FUV ratio. Both data and model are used to estimate and compare the extinction gradients at the FUV wavelength obtained from these various indicators. We discuss the implications for the determination of the star formation rate.

Subject headings: dust, extinction — galaxies: individual (M83) — ultraviolet: galaxies

¹Observatories of the Carnegie Institution of Washington, 813 Santa Barbara St., Pasadena, CA 91101

²NASA/IPAC Extragalactic Database, California Institute of Technology, Mail Code 100-22, 770 S. Wilson Ave., Pasadena, CA 91125

³Laboratoire d'Astrophysique de Marseille, BP 8, Traverse du Siphon, 13376 Marseille Cedex 12, France

⁴California Institute of Technology, MC 405-47, 1200 East California Boulevard, Pasadena, CA 91125

⁵Center for Astrophysical Sciences, The Johns Hopkins University, 3400 N. Charles St., Baltimore, MD 21218

⁶Center for Space Astrophysics, Yonsei University, Seoul 120-749, Korea

⁷Department of Physics and Astronomy, The Johns Hopkins University, Homewood Campus, Baltimore, MD 21218

⁸Space Sciences Laboratory, University of California at Berkeley, 601 Campbell Hall, Berkeley, CA 94720

⁹Laboratory for Astronomy and Solar Physics, NASA Goddard Space Flight Center, Greenbelt, MD 20771

¹⁰Department of Physics and Astronomy, University of California, Los Angeles, CA 90095

1. Introduction

UV and optical observations of galaxies are in general affected by dust extinction. Empirical determinations of the star formation rate in individual galaxies, modeling of the radial properties and color gradients of galaxies (e.g. MacArthur et al. 2004), or estimations of the “cosmic star formation rate history” (e.g. Madau, Pozzetti, & Dickinson 1998) all need to take into account its effects. While detailed radiative transfer calculations self-consistently accounting for the whole SED can be used to estimate this effect (e.g. Popescu et al. 2000, 2004), it is usually done by applying much simpler standard recipes.

These recipes include the following: (a) The Balmer Decrement method. This involves a comparison of the observed $H\alpha/H\beta$ ratio with its predicted value (2.86 for case B recombination, e.g. Osterbrock 1989). Although usually used for $H\alpha$ attenuation, its results can be extrapolated to other wavelengths (e.g. Buat et al. 2002). (b) The UV Spectral Slope method. Meurer, Heckman, & Calzetti (1999, hereafter M99) proposed a relation between the UV extinction and the UV spectral slope β (the continuum spectrum f_λ between 1300 and 2600 Å having a shape of λ^β) in starbursts. Recently, Kong et al. (2004, hereafter K04) computed the equivalent relationship in the GALEX bands. Finally, (c) the TIR/UV luminosity Ratio method (see M99). Radiative transfer models have shown that this ratio is a robust indicator of the UV extinction as it does not depend much on either the geometry or the star formation history (Gordon et al. 2000).

Each of the above methods has its own limitations. The Balmer Decrement Method is affected by systematics caused by uncertainties in the underlying absorption of the stellar populations, and the fact that it concerns only very massive stars and may not represent the extinction affecting older stars. The UV Spectral Slope Method was calibrated for starburst galaxies and may not apply more generally. Moreover, both methods rely on colors determined at similar wavelength, which are quite sensitive to dust radiative transfer effects (Witt, Thronson & Capuano 1992, Witt & Gordon 2000 -hereafter WG2000). Finally, the TIR/UV method is the most reliable, but until the advent of the Infrared Space Observatory (ISO) and now the Spitzer Space Telescope, this method was limited in its application by the low spatial resolution of the IRAS data.

M83 is an interesting laboratory to test the recipes for extinction given the profusion of data available in addition to the GALEX images and for being almost face-on. Models of its stellar content and chemical evolution can be constrained by these data and used to predict the intrinsic properties of the stellar population. An alternative study combining observations from GALEX and ISO of M101 is presented in Popescu et al. (this issue).

2. Observations

GALEX observed M83 for a total of 1352 s on June 07 2003 simultaneously through its FUV and NUV bands (see Fig. 1). From these images we derive the FUV and NUV profiles by azimuthally averaging along ellipses, after masking the stars, and subtracting the sky. The ellipticity and position angle (0.1 and 80°) were taken from Kuchinski et al.(2000). In this paper, the authors presented Ultraviolet Imaging Telescope (UIT) observations of M83. The galaxy was observed by UIT only in the FUV domain, with a slightly better resolution (~ 3 arcsec) than the GALEX one (~ 5 arcsec). The surface-brightness sensitivity limit of the GALEX image is however ~ 2 mag deeper. Our FUV profile is in good agreement with the one published in Kuchinski et al.(2000) but extend to larger radii. The map and radial profile of the UV spectral slope β_{GLX} (computed in the GALEX bands as in K04) are shown in Fig. 1c & 2a, respectively. We estimate 0.15 mag to be the uncertainty in the calibration of the GALEX AB surface brightnesses.

We derive the $H\alpha$ and $H\beta$ profiles from narrow-band imaging ($\text{FWHM} \simeq 60 \text{ \AA}$) in the lines, and adjacent continuum images, all obtained at the Las Campanas Observatory (Chile) 40-inch telescope using the 2048×3150 pixels CCD camera. The main uncertainty in the $H\alpha$ and especially $H\beta$ surface brightness comes from the underlying Balmer absorption that has to be accounted for. In order to estimate this effect, we use a drift-scanning long-slit spectrum of M83 obtained with WFCCD using the blue grism and slit width of 2 arcsec at the 100-inch du Pont telescope also at Las Campanas. Both $H\beta$ absorption and emission were detected along the central ± 4 arcmin of M83. The average underlying absorption at $H\beta$ is 4.2 \AA (with a rms of 1 \AA along the slit). Since the absorption in $H\alpha$ could not be measured, we assumed it to be the same as for $H\beta$ (e.g. Mccall et al. 1985). The adopted value is close to the absorption obtained with the stellar population model described in next section (4 and 5.5 \AA on average at $H\alpha$ and $H\beta$ respectively). We also use the spectroscopic results to estimate the $[\text{NII}]\lambda\lambda 6548, 6584 \text{ \AA}$ contamination and correct $H\alpha$ accordingly using $[\text{NII}]/H\alpha = 0.45$.

Profiles were computed from the 60 and $100 \mu\text{m}$ images obtained by a IRAS-hires request (Rice 1993). The $60 \mu\text{m}$ image was convolved with a gaussian to obtain a resolution similar to the $100 \mu\text{m}$ image (~ 90 arcsec). The two profiles were then combined to compute the TIR surface brightness profile, following Dale et al. (2001). The resolution of the FUV images was degraded in a similar way before computing the TIR/FUV ratios profiles.

3. Models of M83

We use models for the chemical and spectro-photometric evolution of M83 based on Boissier & Prantzos (2000) (BP2000), with an updated star formation law (depending on the angular velocity) determined in Boissier et al. (2003). To compute the SFR, we adopt the rotation curve of Crosthwaite et al. (2002). These models, however, cannot reproduce the observed gaseous profile (taken from Crosthwaite et al. 2002; Lundgren et al. 2004). This is most likely due to the fact that the models do not include radial inflows. There are reasons why such a flow might be present in M83: the strong bar could induce radial motion and the central starburst needs to be supplied with fresh gas. Interaction with NGC 5253 may be responsible for these peculiarities (van den Bergh 1980). We introduce in the models of BP2000 radial inflows of various efficiencies and various starting times. The best models are chosen as the ones reproducing the observed dust-free profiles: total gas, and near-infrared surface brightness of 2MASS. Several models including a flow beginning a few Gyrs ago (1 to 5) produce satisfactory results. In Fig. 2a, we show the profile of the average intrinsic spectral UV slope (β_0 , short-dashed curve), and the range of values (shaded area) obtained with these best-models.¹

4. Extinction maps and profiles

We now consider the “classical” extinction estimators used in extra-galactic studies: (a) The $A(H\alpha)$ extinction obtained from the $H\alpha/H\beta$ ratio (after correction for the Balmer underlying absorption) can be extrapolated to the FUV wavelength. We obtain $A(FUV)=1.4 A(H\alpha)$ by assuming that the color excess of the stellar continuum is 0.44 times the gaseous emission one (see Buat et al. 2002 and references within), and a Galactic extinction curve (for which $A(H\alpha)/E(H\beta - H\alpha)=2.26$). (b) It is common to apply the method of M99 in galaxies with nuclear starbursts like M83. We compute a profile following this assumption (β -starburst, Fig. 2b), adopting the TIR/FUV- β_{GLX} relation computed by K04. (c) Finally, we compute the extinction $A(FUV)$ from the TIR/FUV ratio following Buat et al. (this issue). The result is presented in Fig. 2b. The absence of features in this gradient is due to the low resolution infra-red IRAS observations. To achieve a better spatial resolution taking advantage of the TIR/FUV calibration for $A(FUV)$, we perform a fit (outside the

¹In the central 50 arcsec of the galaxy, the presence of the starburst and of a bulge are not taken into account in the disk model. In the central starburst itself (10 arcsec), the UV spectral slope of the model is artificially changed to the canonical value -2.1 used for the intrinsic slope of a starburst (Calzetti et al. 2000). More details on the models will be given in a forthcoming paper

50 central arcsec of the bulge) providing $A(FUV)=0.86+0.91 (\beta_{GLX}-\beta_0)$ (dotted lines in Fig. 3, shifted to account for the average value of β_0). We use this result to compute a new extinction profile (β -models in Fig.2, middle panel) from the β_{GLX} profile.

The extinction maps (Fig. 1) and the profiles (Fig. 2) show that the extinction is relatively low in the very center (see the hole at the center of the β_{GLX} -map, Fig. 1c), assuming the low values of β_{GLX} in this region indicate low extinction. The extinction (indicated by the various tracers) becomes rapidly high in a circumnuclear region and progressively decreases as we move into the disk of the galaxy. The various indicators show some common structure: the spectral slope β_{GLX} (and the extinction profiles derived from it), as well as the Balmer decrement, show several correlated peaks. One of the most remarkable is located 100 arcsec from the center. Inspection of the images (Fig. 1) show that this radius corresponds to the position of spiral arms where both the star formation rate and the extinction are enhanced with respect to average regions of the galaxy. The β -starburst extinction gives larger values compared to other indicators, i.e. M83 shows lower extinctions (computed from the TIR/FUV ratio) than starburst galaxies for the same value of β . This is in agreement with the deviations with respect to the starburst case already obtained in the LMC (Bell et al. 2002) or in less active galaxies (K04).

We used earlier a purely empirical relation between $A(FUV)$ and $(\beta_{GLX}-\beta_0)$ in M83. Because of the many uncertainties (geometry, β_0 ...), we prefer this to theoretical prescription. In Fig. 3a, we compare our data outside the bulge with two models of WG2000 (adopting for β_0 the value of our best model) to illustrate the dependence on the geometry. We also compare our results with the model of K04 for the birthrate parameter b obtained in our model of M83 ($\log b \simeq 0.2$). We find that it overpredicts $A(FUV)$ by a large amount for any given value of β_{GLX} . Finally, our data are compared to other samples: the fit of K04 for the starbursts of M99 (solid line), and the integrated NUV and TIR selected galaxies of Buat et al. (this issue). The profile of M83 is consistent with the latter, although with slightly larger β_{GLX} . Fig. 3b shows the $A(FUV)/(\beta-\beta_0)$ ratio (where $A(FUV)$ is still determined from TIR/FUV ratio) as a function of radius (the dotted curve indicates the same profile if the extinction derived from $(\beta-\beta_0)$ as discussed previously is used instead of the TIR/FUV ratio). Outside the bulge, $A(FUV)/(\beta-\beta_0)$ has an average value of 1.9 (this value would become 1.2 if the usual $\beta_0=-2.1$ was adopted).

5. Implications for the star formation rate

The FUV surface brightness profile can be transformed into a star formation rate profile using the standard conversion factor of Kennicutt (1998): $SFR (M_\odot \text{ yr}^{-1}) = 1.4 \times 10^{-28} L_{UV}$

($\text{erg s}^{-1} \text{ Hz}^{-1}$). Regardless of the uncertainties affecting this number (see Kennicutt 1998), the FUV profile must be corrected for extinction to obtain a reliable SFR. Fig. 2c shows the SFR profile obtained without extinction correction (lower dotted line), and with various corrections proposed in the previous section². We find that the SFR profile of our best model (stars in Fig. 2c) is in good agreement with the one deduced from the observations with the TIR/FUV correction. This suggests that the star formation law used in our evolutionary models is quite realistic.

The integrated star formation rate also depends on the extinction correction. Owing to multi-wavelength resolved data, we can compute the SFR of M83 inside 300 arcsec according to various assumptions. With no extinction correction, the derived star formation rate is $1 \text{ M}_{\odot} \text{ yr}^{-1}$. Assuming the whole galaxy behaves like a starburst (β -starburst), we obtain $10.1 \text{ M}_{\odot} \text{ yr}^{-1}$. This assumption is probably over-estimating the star formation rate as the starburst is located only in the center. The extinction based on the Balmer decrement gives a SFR of $3.3 \text{ M}_{\odot} \text{ yr}^{-1}$ and the one based on a combination of the TIR/FUV ratio and β_{GLX} profiles provides $3.6 \text{ M}_{\odot} \text{ yr}^{-1}$ (a similar value of $4 \text{ M}_{\odot} \text{ yr}^{-1}$ is obtained from the low-resolution TIR/FUV extinction profile).

To summarize, we used GALEX observations of M83 in combination with other data to compare several extinction indicators (the UV Spectral Slope method giving poor results), and to estimate the effect of extinction on the determination of the SFR. Differences of a factor up to 2.5 are obtained with the various methods. Moreover, we determined an extinction-free SFR profile allowing to check the validity of the SFR law used in evolutionary models. A similar analysis will be applied to a larger number of galaxies observed by GALEX in the future.

GALEX (Galaxy Evolution Explorer) is a NASA Small Explorer, launched in April 2003. We gratefully acknowledge NASA's support for construction, operation, and science analysis for the GALEX mission, developed in cooperation with the Centre National d'Etudes Spatiales of France and the Korean Ministry of Science and Technology. We thank C. Popescu and R. Tuffs for their comments. S.B. thanks the CNES for its financial support.

REFERENCES

Bell, E. F. 2002, *ApJ*, 577, 150

²We also show the SFR profile deduced from the $H\alpha$ surface brightness profile, corrected from $A(H\alpha)$, and it is very similar to the SFR deduced from the FUV. This fact indicates that the current azimuthally averaged SFR is not very different from the SFR averaged over the last 10^8 years.

- Boissier, S., & Prantzos, N. 2000, MNRAS, 312, 398
- Boissier, S., Prantzos, N., Boselli, A., & Gavazzi, G. 2003, MNRAS, 346, 1215
- Buat, V., Boselli, A., Gavazzi, G., & Bonfanti, C. 2002, A&A, 383, 801
- Calzetti, D., Armus, L., Bohlin, R. C., Kinney, A. L., Koornneef, J., & Storchi-Bergmann, T. 2000, ApJ, 533, 682
- Crosthwaite, L. P., Turner, J. L., Buchholz, L., Ho, P. T. P., & Martin, R. N. 2002, AJ, 123, 1892
- Dale, D. A., Helou, G., Contursi, A., Silbermann, N. A., & Kolhatkar, S. 2001, ApJ, 549, 215
- Gordon, K. D., Clayton, G. C., Witt, A. N., & Misselt, K. A. 2000, ApJ, 533, 236
- Kennicutt, R. C. 1998, ARA&A, 36, 189
- Kong, X., Charlot, S., Brinchmann, J., & Fall, S.M., 2004, to appear in MNRAS (K04)
- Kuchinski, L. E., et al. 2000, ApJS, 131, 441
- Lundgren, A. A., Wiklind, T., Olofsson, H., & Rydbeck, G. 2004, A&A, 413, 505
- MacArthur, L.A., Courteau, S., Bell, E., & Holtzman, J., 2004, Accepted in ApJS
- Madau, P., Pozzetti, L., & Dickinson, M. 1998, ApJ, 498, 106
- McCall, M. L., Rybski, P. M., & Shields, G. A. 1985, ApJS, 57, 1
- Meurer, G. R., Heckman, T. M., & Calzetti, D. 1999, ApJ, 521, 64 (M99)
- Osterbrock, D. E. 1989, Mill Valley:University Science Books
- Popescu, C. C., Misiriotis, A., Kylafis, N. D., Tuffs, R. J., & Fischera, J. 2000, A&A, 362, 138
- Popescu, C. C., Tuffs, R. J., Kylafis, N. D., & Madore, B. F. 2004, A&A, 414, 45
- Rice, W., 1993, AJ, 105, 67
- van den Bergh, S. 1980, PASP, 92, 122
- Witt, A. N. & Gordon, K. D. 2000, ApJ, 528, 799 (WG2000)

Witt, A. N., Thronson, H. A., & Capuano, J. M. 1992, ApJ, 393, 611

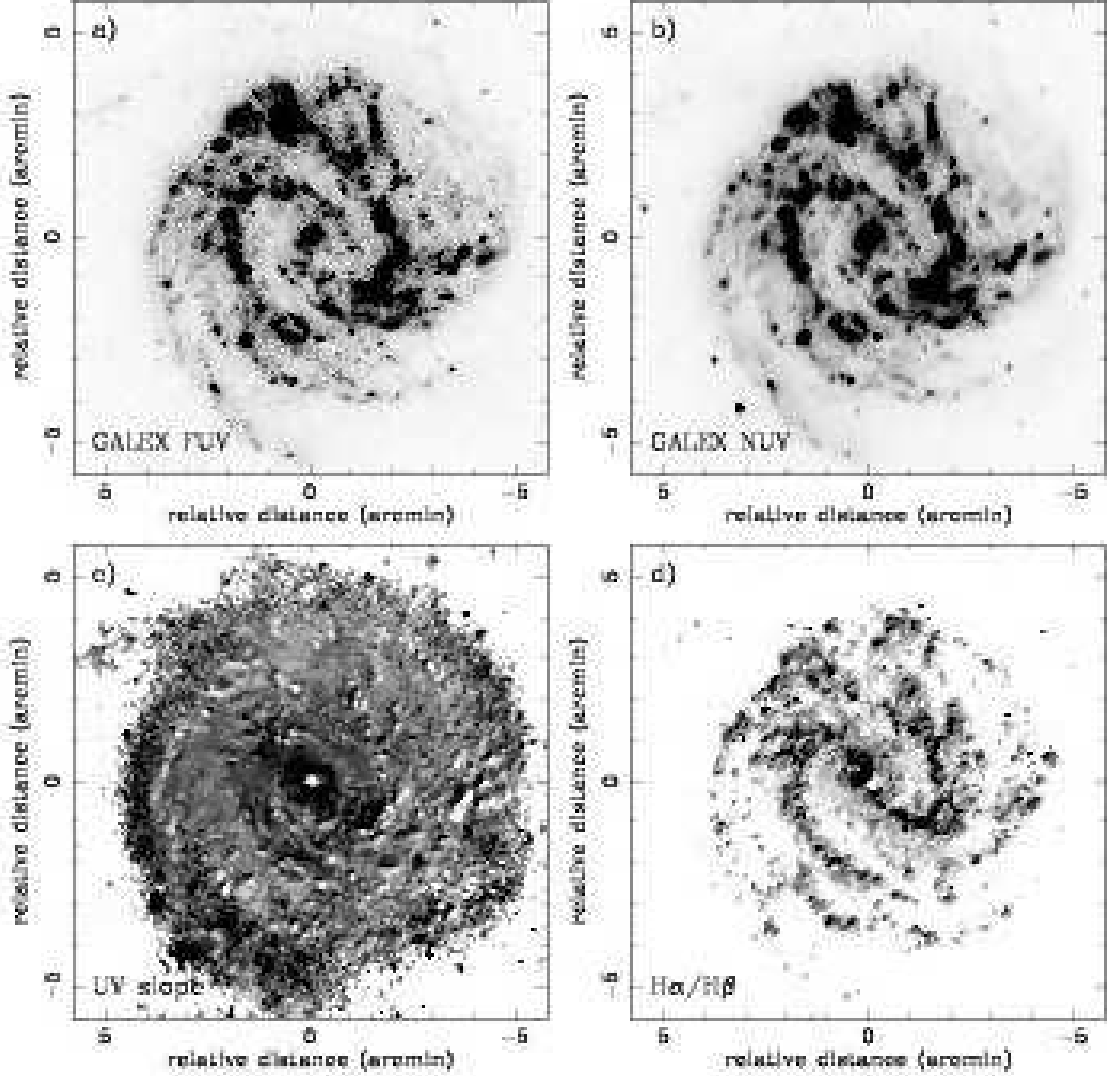


Fig. 1.— *a)* FUV image (from the sky background to 22.3 AB mag arcsec⁻²), *b)* NUV image (from the sky background to 22.7 AB mag arcsec⁻²), *c)* UV spectral slope β , from -2.5 (white) to 0.3 (black). *d)* $H\alpha/H\beta$ ratio, from $H\alpha/H\beta=2$ to 6 . White areas in this plot correspond to regions where either $H\alpha$ or $H\beta$ was below $3\sigma_{\text{sky}}$. A $8'' \times 8''$ median filter was applied in the case of panels *c* & *d*.

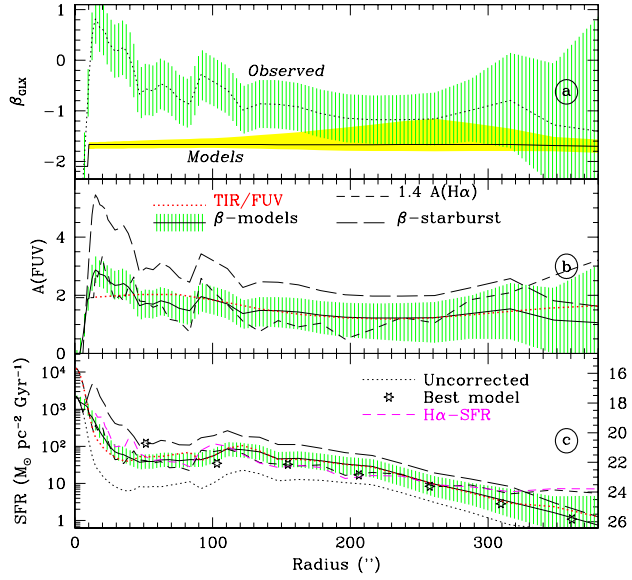


Fig. 2.— *a*) Radial profile of the observed UV spectral slope (dotted, derived from the GALEX bands). The solid curve (shaded area) indicates at each radius the average β_{GLX} (the range of values) obtained with models providing satisfactory profiles. *b*) FUV extinction profiles derived from various indicator (see legend in the figure and details in text). *c*) FUV-deduced Star Formation Rate profiles (surface brightness scale on the right in mag arcsec^{-2}), uncorrected for extinction (dotted), and with the extinction corrections given in panel b. The stars show the current SFR obtained with the model. We also show the SFR deduced from $H\alpha$ corrected for $A(H\alpha)$.

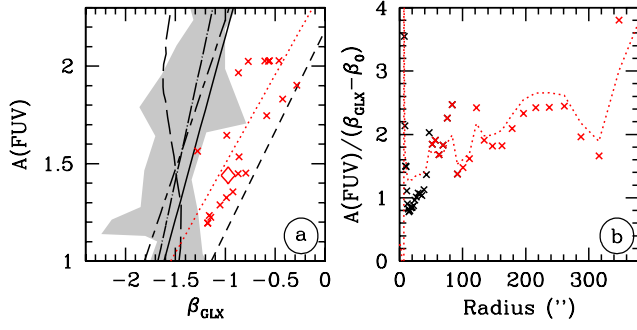


Fig. 3.— *a*) The crosses show the FUV extinction ($A(FUV)$ from the TIR/FUV ratio) as a function of β_{GLX} for our data out of the bulge (i.e. the central 50 arcsec). The dotted line is least-square fit. The shaded area includes the integrated values found by Buat et al. (this issue). The short-long dashed line is the relation found for starbursts in K04. The solid curve is obtained with the model of K04, for a present to past averaged star formation (*b*) such that $\log b=0.2$, typical value obtained with our model of M83. The short and long dashed curves shows the relation expected for different geometrical models of WG2000 (respectively shell-homogeneous and dusty-clumpy). *b*) FUV extinction to $(\beta - \beta_0)$ ratio as a function of radius (crosses). The dotted curve is obtained using the previous fit instead of $A(FUV)$.